Material characterization of segmented polyether poly(urethane–urea–amide)s and its implication in blood compatibility

Kazuhiko Nojima, Kohei Sanui and Naoya Ogata
Department of Chemistry, Faculty of Science and Technology, Sophia University, 7-1 Kioi-cho, Chiyoda-ku, Tokyo 102, Japan

and Nobuhiko Yui, Kazunori Kataoka and Yasuhisa Sakurai
Institute of Biomedical Engineering, Tokyo Women's Medical College, 8-1 Kawada-cho, Shinjuku-ku, Tokyo 162, Japan
(Received 18 April 1986; revised 30 September 1986; accepted 7 October 1986)

The morphology, properties and blood compatibility of segmented polyether poly(urethane–urea–amide)s (AM series) with an aromatic diamine chain extender containing an amide group have been investigated. The AM copolymers exhibited lower moduli than the conventional segmented polyether poly(urethane–urea)s (MT series), although both series showed similar degrees of phase separation between the soft and hard segments. Electron spectroscopy for chemical analysis (e.s.c.a.) revealed that the AM copolymers had a different anisotropy of surface chemical composition for the soft and hard segments at a certain depth, compared with the MT copolymers. The relationship between e.s.c.a. measurements and platelet adhesion to the copolymer surface showed that platelet adhesion was minimized for a copolymer whose hard-segment domain had a particular surface nature. These results suggest that surface morphology, particularly the size of the hard-segment domains on the copolymer surface, has a specific effect on suppressing platelet adhesion, which could lead to the molecular design of novel antithrombogenic materials.

(Keywords: blood compatibility; segmented polyether poly(urethane–urea–amide); phase separation; electron spectroscopy for chemical analysis; hard-segment domain)

INTRODUCTION

Recently, the development of excellent antithrombogenic materials has been required due to progress in the investigation of artificial organs[1]. It is a fact that these materials must have excellent antithrombogenicity and mechanical properties, especially for use in artificial hearts and surgical prostheses. Thus segmented polyether–poly(urethane–urea) (PEUU), commercially available as Biomer®, has been widely used in such applications[2,3]. Moreover, many studies concerned with PEUUs have been done mainly to explain their antithrombogenicity in relation to material characterization[4–8]. PEUU is a multi-block copolymer of alternating sequences of soft and hard segments. The hard segment shows strong intermolecular hydrogen bonding and aggregates into paracrystal-like domains, while the soft segment forms matrices surrounding the hard-segment domains.

We have carried out studies on the blood compatibility of segmented copolymers in relation to their morphology and properties[9–16]. In our previous studies on segmented polyether poly(urethane–urea–amide)s (PEUUAs) chain extended by an aliphatic diamine containing amide groups, we reported that PEUUAs showed a suppressive effect on blood platelet adhesion to the copolymer surface and an increase in mechanical properties (strength and modulus): the mechanical properties of copolymers were improved by incorporation of amide groups into the hard segments, although the degree of phase separation between the soft and hard segments depended primarily upon the molecular weight of the soft segment[12].

In this study, in order to investigate the effect of the hard segment on the properties, stucture and blood compatibility, we synthesized segmented polyether poly(urethane–urea–amide)s (AM series) by using an aromatic diamine containing an amide group, and examined the physicochemical properties in terms of the relationship between surface chemical composition of the copolymers and platelet adhesion to the copolymer surface.

0032-3861/87/061017-08$03.00

EXPERIMENTAL

Preparation of reagents

Poly(propylene oxide) (PPO) of number-average molecular weight ($\bar{M}_n$) 1040, 1170, 1450 and 1960 (supplied by Asahi Denka Kogyo Co. and Dai-ichi Kogyo Seiyaku Co.) were dehydrated *in vacuo* at 60°C for 48 h. *p*-Nitrobenzoyl chloride, 4,4′-diphenylmethane diisocyanate (MDI), *N*,*N*′-dimethylacetamide (DMAc) and *N*-methyl-2-pyrrolidone (NMP) were purified by distillation. *p*-Nitroaniline and 4,4′-diaminodiphenylmethane (DAM) were recrystallized from benzene.

Preparation of 4,4′-diaminobenzanilide (DABA)

One mole of *p*-nitrobenzoyl chloride solution in DMAc was added to two moles of *p*-nitroaniline dissolved in DMAc. The reaction mixture was stirred at about 20°C for 5 h. The mixture was poured into water, and the precipitate was recrystallized from acetone. The product was suspended in a 1:2 mixture of HCl and ethanol, followed by adding a 45 wt% stannous chloride solution in ethanol. After reacting at 60°C for 10 h, the mixture became a transparent yellow solution. The reaction mixture was cooled down to 0°C in order to recrystallize DABA. The DABA was dissolved in water, and 10 wt% NaOH solution was added dropwise to give a yellow precipitate. The product was then dried *in vacuo* at 40°C for 48 h to give a yellow powder (m.p. 212°C, yield 31.7%).

Preparation of segmented polyether poly(urethane–urea–amide)

The AM copolymers used in this study were synthesized by the prepolymer method shown below.

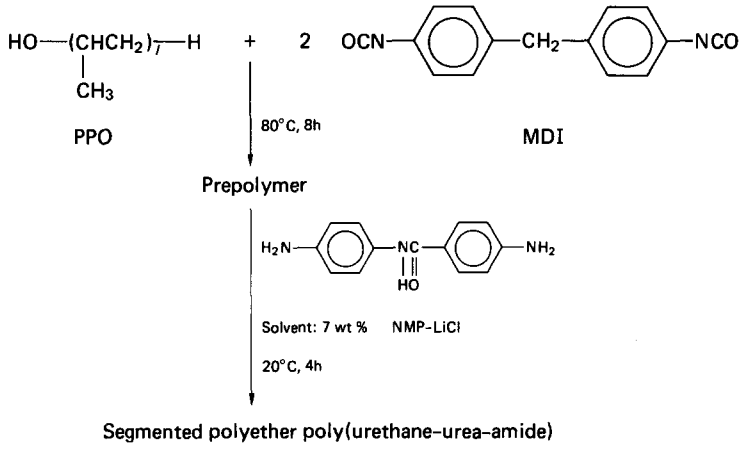

PPO and MDI were placed in a four-necked, round-bottomed flask equipped with a stirrer, a drying tube and a dropwise funnel. After reacting at 80°C for 8 h, the mixture was cooled to room temperature and a 7 wt% LiCl–NMP solution of DABA (5 wt%) was added to the flask. The reaction mixture was stirred at about 20°C for 4 h. The entire synthesis was performed under a continuous purge of dry nitrogen. The molar ratio of MDI, PPO and DABA was 2:1:1. The polymers obtained were precipitated in methanol, and then dried *in vacuo* for a week. Control samples of the conventional MT series were also prepared by the above procedure, except using DAM as chain extender. The structural formulae of AM and MT copolymers are shown below.

Soft segment

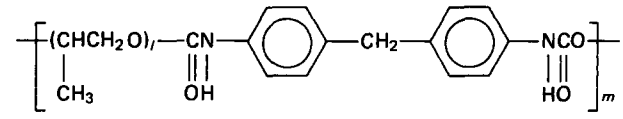

Hard segment

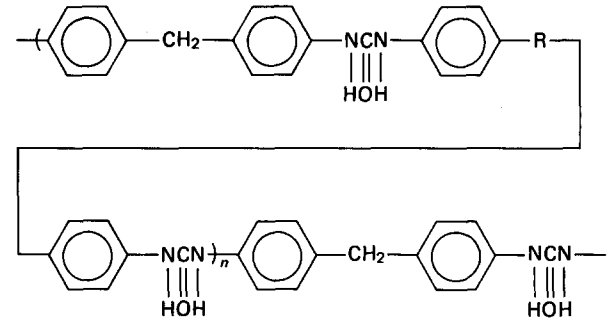

R = -CN- (AM), $-CH_2-$ (MT)
OH

For convenience, AM and MT copolymers will be designated by a two-sequence code, such as AM-1040, where 1040 refers to the $\bar{M}_n$ of the PPO segment.

Film preparation

Films for various measurements were prepared by casting a *m*-cresol solution of polymer (5 wt%) onto glass plates, followed by evaporating the solvent at 70°C. The films obtained were dried completely *in vacuo* at 60°C for 48 h.

Dynamic mechanical measurement

Measurement was made on a Vibron Dynamic Viscoelastometer (Toyo Baldwin, Reovibron DDV-II-B). The temperature range was from −120°C to 120°C under a dry nitrogen atmosphere and the frequency employed was 11 Hz. The sample films were prepared by the procedure described above.

Tensile properties

Uniaxial stress–strain experiments were made with a Shimadzu Autograph IS-5000 at room temperature, with a crosshead speed of 300 mm min^{-1} and initial gauge length of 17 mm. The sample films were made according to the above procedure.

Differential scanning calorimetry (d.s.c.)

D.s.c. thermograms from −120°C to 160°C were obtained using a differential scanning calorimeter (Rigakudenki 8085) at a heating rate of 20°C min^{-1}. The sample films were made according to the above procedure.

Electron spectroscopy for chemical analysis (e.s.c.a.)

E.s.c.a. spectra were obtained on an ESCA 750 photoelectron spectrometer (Shimadzu Co.) employing a magnesium anode (Mg Kα = 1253.6 eV) which was operated at 8 kV and 30 mA. Samples were generally mounted with double-sided sticky tape, and the operation

was run under evacuation to $(1–4) \times 10^5$ Pa at 25°C. The charging shift was referred to the C_{1s} line emitted from neutral carbon at 285.0 eV. The emission angle of photoelectrons was varied in the range from 15° to 90° in order to obtain the depth–composition profiles on these copolymer surfaces.

Estimation of platelet adhesion[17]

One gram of copolymer-precoated glass beads (48–60 mesh) was closely packed in poly(vinyl chloride) tubing (inner diameter 3 mm) equipped with a stopcock. The packed column was primed with saline and subjected to the following platelet adhesion test: 3 cm^3 of fresh blood was collected from a jugular vein of a mongrel dog with a disposable syringe without use of any anticoagulant. The blood was immediately passed through the column for 60 s at a flow rate of 1.2 $cm^3\,min^{-1}$ using a Precidol 5003 infusion pump. The eluted blood was collected in a sample bottle containing 0.1 cm^3 of 4 wt% aqueous solution of sodium citrate as anticoagulant. Platelet counts in the eluted blood were performed with a haemacytometer according to the method of Brecher and Cronkite, in order to determine the amount of platelets adhering to the copolymer surface.

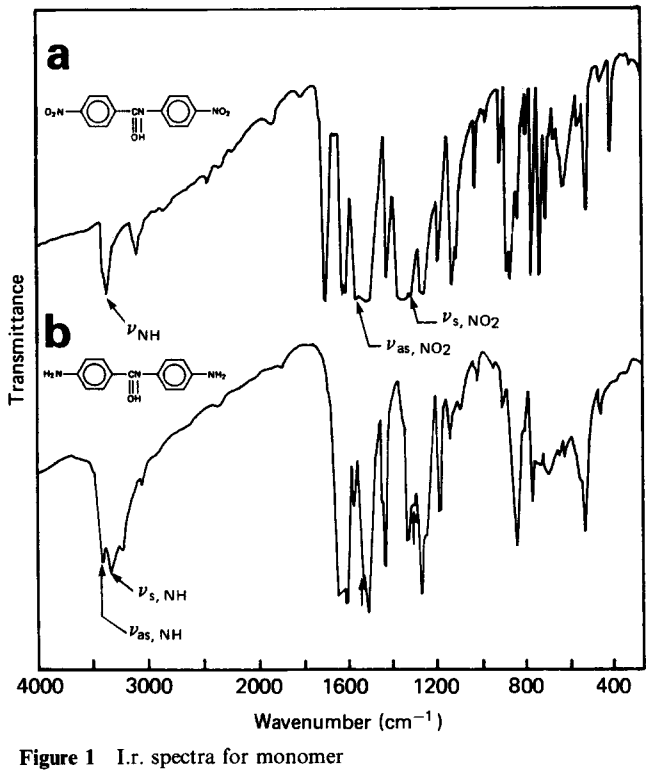

Figure 1 I.r. spectra for monomer

RESULTS AND DISCUSSION

Preparation of polymer

Figure 1 shows i.r. spectra of DABA. DABA showed main peaks at 3400 cm^{-1} and 3350 cm^{-1} due to δ NH, 1640 cm^{-1} due to ν C=O and 1570 cm^{-1} due to δ NH. The peak due to the nitro group in *Figure 1a* disappeared by reduction, and a peak due to δ NH appeared at 3400 cm^{-1} in *Figure 1b*.

Results of the polymerization are summarized in *Table 1*. The results of elemental analysis were in close agreement with the expected values. These results support the conclusion that the prepared AM copolymers have the designated structure chain-extended by DABA.

Kimura *et al.*[18] reported that segmented polyurethanes having poly(tetramethylene oxide) (PTMO) as soft segment and DAM as chain extender had a soft-segment domain of size 0.4–2.4 nm, dependent upon M_n of PTMO, and a hard-segment domain of size 9.3 nm. From the result that the Bragg spacings of AM copolymers were basically identical to those of MT copolymers, the difference in hard-segment length between AM and MT copolymers could be neglected. Therefore, both AM and MT copolymers are considered to show a similar soft-segment M_n dependence of the size of the soft- and hard-segment domains as Kimura's copolymers.

Temperature dependence of dynamic viscoelasticity

Figure 2 shows the temperature dependences of the storage (E') and loss (E'') moduli of AM and MT copolymers. Both figures exhibit a mechanical relaxation

Table 1 Synthesis of segmented polyether polyurethanes

Sample		Elemental analysis (wt%) C	H	N	Amount of hard segment[a] (wt%)	η_{sp}/c [b] (dl g^{-1})	Yield (%)
AM-1040	found	64.78	8.27	5.34	27.9	0.57	81.2
	calc.	65.03	8.06	5.54			
AM-1170	found	64.12	8.69	4.41	29.1	0.66	66.1
	calc.	64.83	8.22	5.16			
AM-1450	found	64.47	8.99	4.78	20.7	0.64	61.5
	calc.	64.47	8.50	4.50			
AM-1960	found	64.11	9.26	3.45	18.9	0.78	36.6
	calc.	64.02	8.85	3.64			
MT-1040	found	65.33	8.58	4.86	26.3	1.92	96.7
	calc.	66.19	8.15	4.83			
MT-1170	found	65.49	9.04	4.32	23.2	2.45	93.0
	calc.	65.90	8.31	4.50			
MT-1450	found	65.38	9.04	3.90	20.8	1.38	85.6
	calc.	65.40	8.57	3.91			
MT-1960	found	62.76	9.52	3.86	21.3	1.30	86.5
	calc.	64.76	8.91	3.16			

[a] Weight fraction of hard segment in copolymer was determined by elemental analysis
[b] 0.1 g/10 cm^3 in *m*-cresol at 30°C

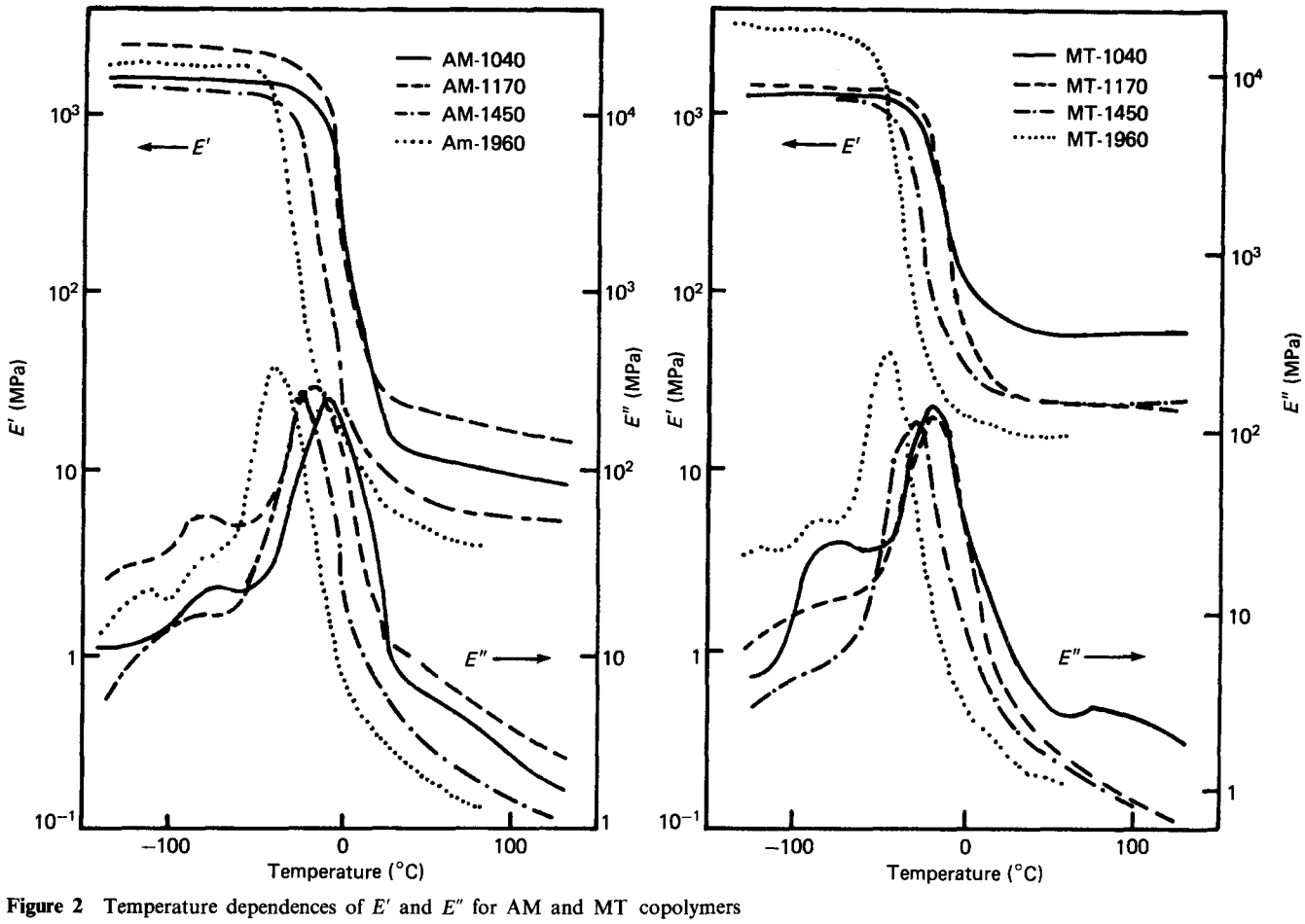

Figure 2 Temperature dependences of E' and E'' for AM and MT copolymers

region, which is attributed to micro-Brownian motion of the soft segment accompanying its glass transition temperature (T_g), in each copolymer. *Table 2* shows the results of T_g determined by d.s.c. and from the loss peak in E''. The T_g of AM copolymers varied with the $\bar{M}_n$ of the soft segment, which was similar to that of MT copolymers. These results indicate that both AM and MT copolymers exhibit phase separation between the soft and hard segments, the degree of which was dependent on the $\bar{M}_n$ of the soft segment. However, it is of interest that the magnitude of E' for AM copolymers in the plateau region (above room temperature) was lower than that for MT copolymers. Thus we found that AM copolymers were softened by substituting methylene groups for amide groups in its hard segments, independent of the degree of phase separation between the soft and hard segments. Presumably the density of physical crosslinks for AM copolymers was lower than that for MT copolymers.

Stress–strain behaviour

The stress–strain curves of AM and MT copolymers are shown in *Figure 3*. AM copolymers exhibited lower moduli and strengths than MT copolymers. The behaviour of the modulus was consistent with the results of dynamic viscoelasticity. The lower elongation at break for AM copolymers is considered to be due to the low $\bar{M}_n$ of AM copolymers, which can be seen in terms of polymer viscosity in *Table 1*.

It is a characteristic of the molecular design of AM copolymers that the hard segment consists of an alternating copolymer of amide and urea groups. In general, it is reported that an alternating copolymer in

Table 2 D.s.c. and Reovibron data

Sample	D.s.c. T_g (range) (°C)	D.s.c. ΔT_g (°C)	Vibron T_g (°C)
AM-1040	−12 (−24 to 0)	24	−7.5
AM-1170	−20 (−28 to 0)	28	−12.0
AM-1450	−30 (−39 to −15)	24	−23.6
AM-1960	−45 (−63 to −10)	53	−42.6
MT-1040	−15 (−16 to 0)	16	−10.1
MT-1170	−28 (−30 to −4)	26	−16.7
MT-1450	−38 (−50 to −10)	40	−29.8
MT-1960	−50 (−52 to −24)	28	−50.9

which the functional groups are regularly arranged shows advantages such as high melting temperature, high crystallinity and high mechanical strength, whereas a copolymer having an irregular arrangement exhibits a different tendency in such properties[19–21]. These results suggest that copolymer properties depend primarily upon the regularity of arrangement of the functional groups in repeat units. Previously, we reported that the mechanical properties of PEUUA chain-extended by an aliphatic diamine containing two amide groups exhibited higher modulus and strength than conventional PEUU[12]. However, the moduli of AM copolymers were lower than those of MT copolymers, and this result was not consistent with our previous result. We consider that this contradiction would cause a difference in arrangement of the functional groups in the hard segment. The hard segment of PEUUA has a repeat unit composed of two amide and two urea groups, that is, an even–even number

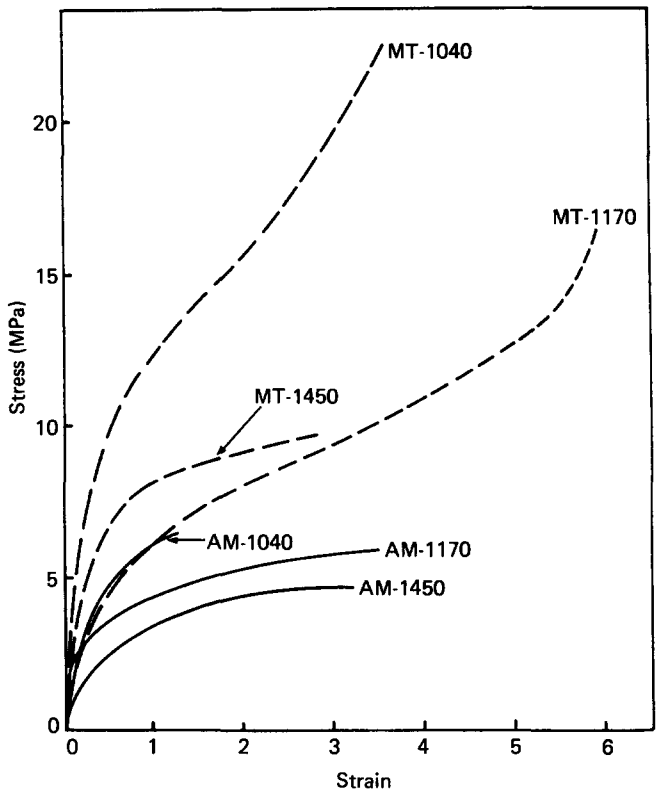

Figure 3 Stress–strain curves for AM and MT copolymers

arrangement of different functional groups, while the hard segment of AM copolymers has a repeat unit composed of one amide and two urea groups, an odd–even number arrangement of functional groups. Thus it is considered that the introduction of amide groups in AM copolymers would cause an irregular arrangement of functional groups, which is directly connected with a decrease in intermolecular hydrogen bonding, resulting in the reduction of such properties as strength and modulus.

Surface chemical composition

Recently, progress in the analysis of outermost surfaces has been remarkable, with advanced spectroscopic techniques such as e.s.c.a.[22–26] Much information on the chemical composition within ~5 nm of the surface and subsequent microstructure can be obtained quantitatively by e.s.c.a. In this study, in order to obtain the depth–chemical composition profiles of the copolymer surfaces, we performed angular-dependent e.s.c.a. measurements by tilting the surface of samples so that the emission angle of photoelectrons would decrease with respect to the direction of the analyser. Thus from the electron mean-free-path length, $\lambda_e = 1$–2 nm, the sampling depth d, at emission angle θ, is given by $3\lambda_e \sin\theta$, which will be approximately 1–6 nm, corresponding to $\theta = 15$ to $\theta = 90°$. *Figure 4* shows the emission-angle dependence of e.s.c.a. spectra on AM-1450. All spectra show three carbon peaks, one nitrogen peak and one oxygen peak. The C_{1s} peaks corresponding to the aliphatic and aromatic carbons, and to the ethereal carbon were observed at 285.0 eV and 286.5 eV, respectively. The C_{1s} peak corresponding to the carbonyl carbon of urethane, urea and amide groups was observed as a small shoulder near 288.8 eV. The N_{1s} peak was located at approximately 400 eV corresponding to the nitrogen of urethane, urea and amide groups. The O_{1s} peak appeared at around 533 eV mainly corresponding to ethereal oxygen.

Figure 5 shows the relation between the $\bar{M}_n$ of PPO and the ratio of oxygen to nitrogen atoms (O/N), evaluated from the e.s.c.a. spectra (full curve) and elemental analysis in bulk (broken line). The O/N value changes proportionally with an increase in $\bar{M}_n$ of PPO; therefore, O/N evaluated from the e.s.c.a. measurement would represent the relative concentration of PPO segments on the polymer surface. Although both AM and MT copolymers showed similar PPO $\bar{M}_n$ dependences of O/N, MT copolymers showed higher O/N values than the corresponding AM copolymers.

The emission-angle dependences of O/N of AM and MT copolymers are shown in *Figure 6*. In the AM and MT series, the magnitude of O/N increased on approaching the surface. This result could be explained in the following way: concentration of the component with lower surface energy (PPO) occurs on the air-facing surface, resulting in the formation of a thermodynamically stable surface. Thus the anisotropy of chemical composition with depth was studied in terms of the varying $\bar{M}_n$ of PPO. The relation between $\bar{M}_n$ of PPO and the difference in O/N at $\theta = 15°$ and $\theta = 90°$, Δ(O/N), was examined and is shown in *Figure 7*. Here Δ(O/N) indicates a parameter of anisotropic chemical composition at a certain sample depth. Both AM and MT copolymers showed a positive value, which increased with increase in $\bar{M}_n$ of PPO. These results indicate that, in the case of low $\bar{M}_n$ of PPO, the soft and hard segments in the copolymer would be partially mixed due to imperfect

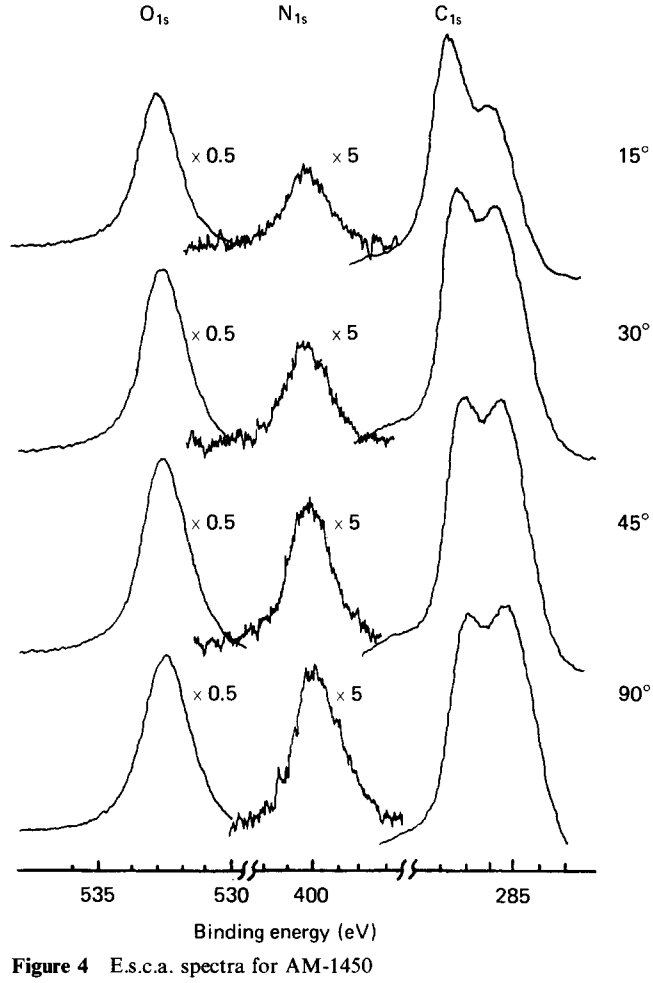

Figure 4 E.s.c.a. spectra for AM-1450

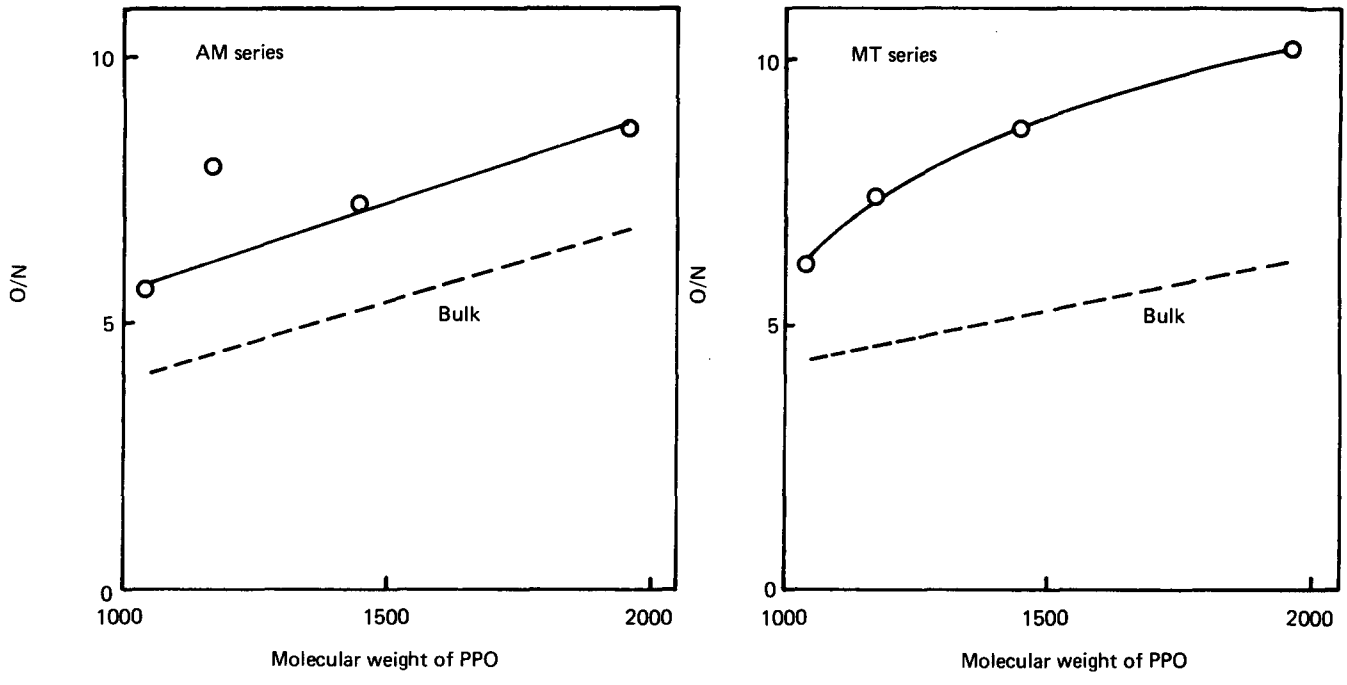

Figure 5 Relation between $\bar{M}_n$ of PPO and O/N at $\theta = 90°$ for AM and MT copolymers

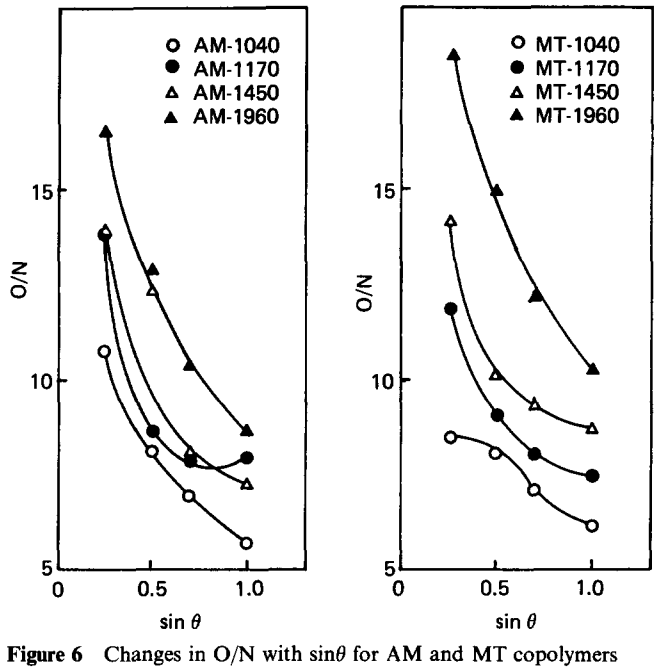

Figure 6 Changes in O/N with sinθ for AM and MT copolymers

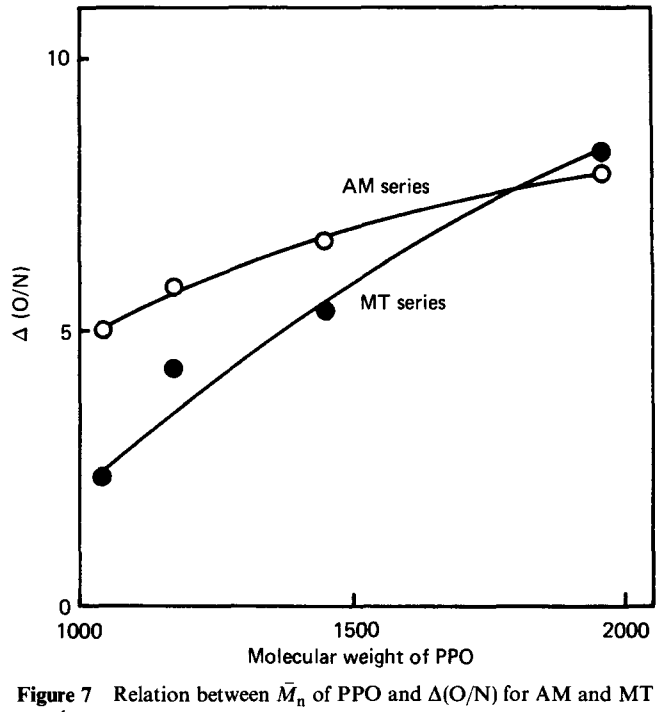

Figure 7 Relation between $\bar{M}_n$ of PPO and Δ(O/N) for AM and MT copolymers

phase separation, whereas, in the case of higher $\bar{M}_n$ of PPO, the concentration of the soft segments would be enhanced because of inhibiting hard segment mixing into soft segments. However, in the PPO $\bar{M}_n$ dependence of Δ(O/N), AM copolymers showed a higher Δ(O/N) over a wide range of PPO $\bar{M}_n$. Perhaps this result indicates that the difference in anisotropic distribution of soft and hard segments exists over a certain depth between AM and MT copolymers, which have almost the same bulk structure with respect to the degree of phase separation and the domain size of soft and hard segments.

Thus there may be an issue whether any other microstructure, apart from the bulk structure, exists on the outermost surface of the copolymers. At first, the possibility of a thin overlayer of PPO segments existing at the surface could be neglected because one did not observe the PPO concentration to increase exponentially when lowering the emission angle of photoelectrons. Consequently, the concentration effect of PPO segments can be explained by saying that the PPO segments would partially screen the hard-segment domains, resulting in diminishing the apparent size of the hard-segment domains at the surface. Therefore, the difference in Δ(O/N) between AM and MT copolymers may argue for the existence of discrete surface microstructure with respect to the hard-segment domains.

Blood compatibility

Blood compatibility of copolymers was evaluated by estimating platelet adhesion to the copolymer surface.

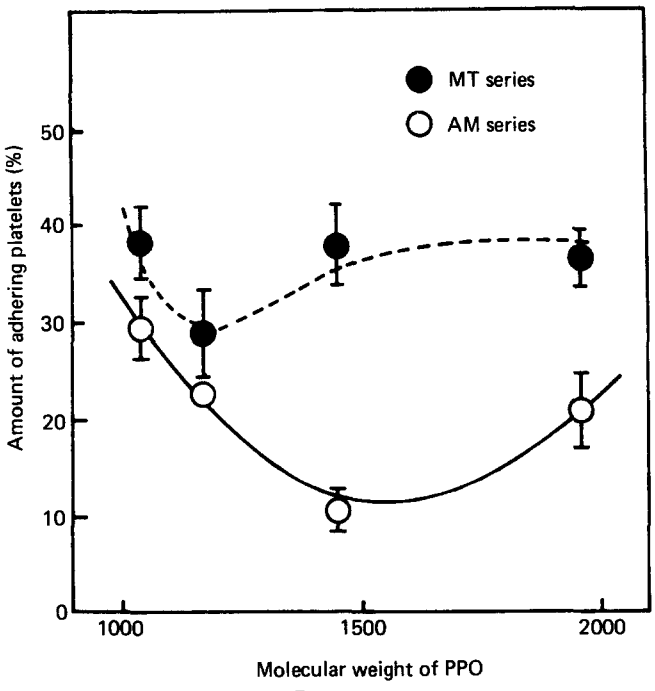

Figure 8 Relation between $\bar{M}_n$ of PPO and amount of adhering platelets for AM and MT copolymers (bars represent standard error of mean)

The adhesion behaviour of platelets on copolymer surfaces was examined in six dogs, and the average and standard error of mean for the platelet counts were calculated to determine the amounts of adhering platelets. *Figure 8* shows the relationship between platelet adhesion to the copolymer surface and the $\bar{M}_n$ of PPO used in the copolymers. MT copolymers showed adhering platelets of 30–40% in whole blood. In the case of AM copolymers, the amount of adhering platelets was in the range of 10–30%; AM-1450 especially exhibited an excellent suppressive effect on platelet adhesion.

Both series showed an optimum $\bar{M}_n$ of PPO, that is, optimum ratio of soft/hard segments, for minimizing platelet adhesion. Therefore, we considered that platelet adhesion might be suppressed through an optimum surface nature of soft and hard segments. Thus, the results of the e.s.c.a. measurement were examined in relation to platelet adhesion to the copolymer surface. *Figure 9* shows the variation of platelet adhesion with O/N for copolymers. As *Figure 9* shows, the suppressive effect on adhering platelets could not be explained by the O/N value. The O/N value represents the amount of polyether on the copolymer surface and the relative size of the soft-segment domains at the surface. On the other hand, considering those copolymers having similar size hard-segment domains in the bulk, independent of $\bar{M}_n$ of PPO, the size of the hard-segment domains at the copolymer surface might prescribe how the hard-segment domains were screened with polyether. Thus the difference in O/N between the outermost surface and the inner region, Δ(O/N), may reflect the relative value of the hard-segment domain size on the copolymer surface. *Figure 10* shows the variation of Δ(O/N) with platelet adhesion to the copolymer surface. The amount of adhering platelets was a minimum for the copolymer having Δ(O/N)=6.5, which might show the existence of an optimum hard-segment domain size on the copolymer surface for suppressing platelet adhesion. Therefore, we suggest that platelet adhesion to the segmented polyurethane surface may be connected with surface microstructure, especially the size of the hard-segment domains on the copolymer surface.

CONCLUSION

A series of segmented polyether poly(urethane–urea–amide)s with aromatic diamine chain extender containing an amide group were synthesized and their morphology and properties were characterized. Also, the blood compatibility of these copolymers was investigated in

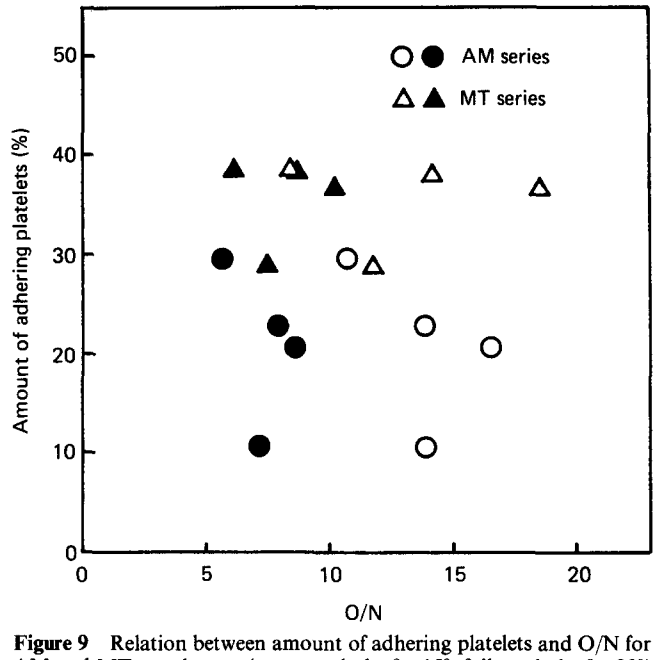

Figure 9 Relation between amount of adhering platelets and O/N for AM and MT copolymers (open symbols, $\theta=15°$; full symbols, $\theta=90°$)

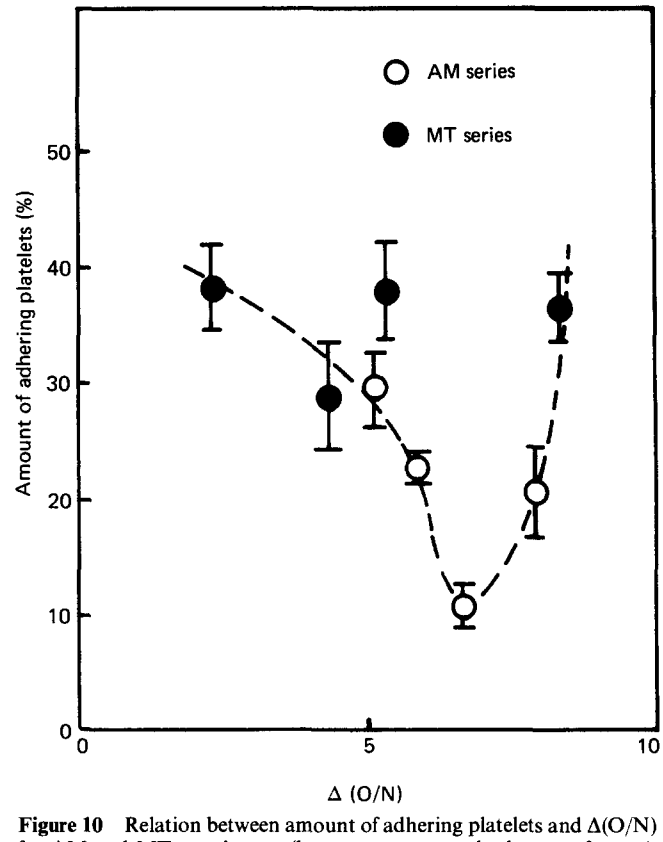

Figure 10 Relation between amount of adhering platelets and Δ(O/N) for AM and MT copolymers (bars represent standard error of mean)

terms of the relationship between blood platelet adhesion and outermost chemical composition. The modulus was reduced by the introduction of amide groups into the hard segments. This result is attributed to the irregular arrangement of the hard segment. E.s.c.a. measurements revealed that these copolymers showed an increase in surface anisotropy of composition of the soft and hard segments. In the blood compatibility of the copolymers, the amount of adhering platelets showed a minimum for the copolymer having $\Delta(O/N)=6.5$, depending on the surface anisotropy of the copolymer. This result indicates that the degree of screening of hard-segment domains by soft segments, that is, the size of the hard-segment domains on the copolymer surface, is one of the important factors in realizing an antithrombogenic surface.

ACKNOWLEDGEMENTS

The authors are grateful to Professor Dr Tisato Kajiyama and Associate Professor Dr Atsushi Takahara, Kyushu University, for their advice and assistance in carrying out the dynamic mechanical measurement and the e.s.c.a. measurement. Sincere thanks are due to Mr Fumio Keitoku, Miss Chiaki Ikeda and Mr Takashi Aoki, Sophia University, for their active collaboration in the course of this study. This study was financially supported by the Ministry of Education, Science and Culture, Japan (Special Project Research, 'Design of Multiphase Biomedical Materials') and by the Japan Research Promotion Society for Cardiovascular Diseases.

REFERENCES

1 Joyce, L. D., DeVries, W. C., Hastings, W. L., Olsen, D. B., Jarvik, M. D. and Kolff, W. J. *Trans. ASAIO* 1983, **29**, 81
2 Lelah, M. D., Lambrecht, L. K., Young, B. R. and Cooper, S. L. *J. Biomed. Mater. Res.* 1983, **17**, 1
3 Wilkes, G. L., Dziemianowicz, T. S. and Ophir, Z. H. *J. Biomed. Mater. Res.* 1979, **13**, 9
4 Lyman, D. J., Kwann-Gett, C., Zwart, H. H. J., Blant, A., Eastwood, N., Kawai, J. and Kolff, W. J. *Trans. ASAIO* 1971, **17**, 456
5 Boretos, J. M., Pierce, W. S., Baire, R. E., LeRoy, A. F. and Donachy, H. J. *J. Biomed. Mater. Res.* 1975, **9**, 327
6 Takahara, A., Tashita, J., Kajiyama, T., Takayanagi, M. and MacKnight, W. J. *Polymer* 1985, **26**, 987
7 Takahara, A., Tashita, J., Kajiyama, T., Takayanagi, M. and MacKnight, W. J. *Polymer* 1985, **26**, 979
8 Hayashi, K., Matsuda, T., Tanaka, H., Umezu, M., Taenaka, Y. and Nakamura, T. *Biomaterials* 1985, **6**, 82
9 Yui, N., Tanaka, J., Sanui, K., Ogata, N., Kataoka, K., Okano, T. and Sakurai, Y. *Polym. J.* 1984, **16**, 119
10 Yui, N., Tanaka, J., Sanui, K. and Ogata, N. *Makromol. Chem.* 1984, **185**, 2259
11 Yui, N., Oomiyama, T., Sanui, K., Ogata, N., Kataoka, K., Okano, T. and Sakurai, Y. *Makromol. Chem., Rapid Commun.* 1984, **5**, 805
12 Yui, N., Nojima, K., Sanui, K. and Ogata, N. *Polym. J.* 1985, **17**, 969
13 Nojima, K., Yui, N., Sanui, K., Ogata, N., Kataoka, K., Okano, T. and Sakurai, Y. *Jpn. J. Artif. Organs* 1985, **14**, 750
14 Yui, N., Sanui, K., Ogata, N., Kataoka, K., Okano, T. and Sakurai, Y. *J. Biomed. Mater. Res.* 1986, **20**, 929
15 Yui, N., Kataoka, K., Sakurai, Y., Sanui, K., Ogata, N., Takahara, A. and Kajiyama, T. *Makromol. Chem.* 1986, **187**, 943
16 Yui, N., Kataoka, K., Sakurai, Y., Keitoku, F., Sanui, K. and Ogata, N. *Makromol. Chem.* 1986, **187**, 1389
17 Kataoka, K., Akaike, T., Sakurai, Y. and Tsuruta, T. *Makromol. Chem.* 1978, **179**, 1121
18 Ishihara, H., Kimura, I., Saito, K. and Ono, H. *Rep. Prog. Polym. Phys. Jpn.* 1970, **13**, 409
19 Preston, J. and Black, W. B. *J. Polym. Sci.* 1965, **B3**, 845
20 Preston, J. and Dobinson, F. *J. Polym. Sci.* 1964, **B2**, 845
21 Preston, J. *ACS Polym. Prepr.* 1961, **6**, 42
22 Graham, S. W. and Hercules, D. M. *J. Biomed. Mater. Res.* 1981, **15**, 465
23 Paik Sung, C. S. and Hu, C. B. *J. Biomed. Mater. Res.* 1979, **13**, 161
24 Ratner, B. D. *Ann. Biomed. Eng.* 1983, **11**, 313
25 Costa, V. S. D., Russell, D. B., Salzman, E. W. and Merrill, E. W. *J. Colloid Interface Sci.* 1981, **80**, 445
26 Takahara, A. and Kajiyama, T. *Nippon Kagaku Kaishi* 1985, 1293